Progress In Electromagnetics Research Letters, Vol. 7, 59–68, 2009

ANALYSIS OF A HIGH-GAIN FABRY-PÉROT CAVITY ANTENNA WITH AN FSS SUPERSTRATE: EFFECTIVE MEDIUM APPROACH

D. Kim and J. I. Choi

Electromagnetic Future Technology Research Team
Electronics and Telecommunications Research Institute
138, Gajeongno, Yuseong-gu, Daejeon, 305-700, Korea

Abstract—A new approach to analyze the behavior of a Fabry-Pérot cavity type high-gain antenna covered with a frequency selective surface (FSS) superstrate is presented. Using an image theory and effective constitutive parameter retrieval, properties of impedance and a refractive index of the entire cavity structure are investigated. Through the analysis, we show that our antenna inherently operates in the medium whose maximum magnitude of the refractive index is lower than '0.5'.

In consequence, we demonstrate that the high-gain feature of the Fabry-Pérot cavity antenna is not only due to satisfy a conventional cavity resonance condition, but also for a wave collimation effect of a metamaterial with the effectively low index of refraction. To show the collimation effect of the cavity, phase properties of a radiating wave with and without the FSS superstrate are examined. Moreover, the effect of the real and imaginary parts of the refractive index on behaviors of the antenna is also investigated by analyzing the derivative of a realized gain of the antenna within an impedance matched frequency band.

1. INTRODUCTION

Conventional way to obtain a high-gain and high-directivity antenna is forming an antenna array with appropriate feeding networks. But, intricate feeding mechanisms to meet suitable phase delays make the antenna system complicated and they also cause unwanted signal losses.

Corresponding author: D. Kim (dhkim@etri.re.kr).

To overcome those problems, an antenna covered with a photonic bandgap (PBG) resonator superstrate, which requires about half-wavelength separation between the antenna and the superstrate, was proposed and it showed a high-gain and high-directivity with only a single feeder [1]. Later, the PBG-type superstrate was substituted with a frequency selective surface (FSS) that was able to control a reflection phase of the superstrate resulting in a resonance length reduction between the superstrate and a ground plane [2, 3]. Antenna resonating at multiple frequency bands was also reported in [4], which equipped with a superstrate composed of double dielectric slabs of different dielectric constants. Electronically reconfigurable high-gain antenna covered with a partially reflective surface (PRS) superstrate, and various antenna arrangement methods to effectively enhance a gain of the antennas located inside a Fabry-Pérot cavity were also proposed [5–7].

One of established ways to predict the performance of an antenna covered with a phase-controllable superstrate (PCS) such as PBG, FSS, and PRS is to find a resonance condition inside a cavity composed of a superstrate and a substrate. In general, this resonance condition analysis method provides a good approximation at a resonant frequency. However, it does not fully explain the high-gain feature around the resonant frequency region. Therefore, to more precisely demonstrate an enhanced overall performance of cavity-resonance antennas covered with a PCS, the physical properties of the cavity itself should be examined.

For that reason, we reinvestigate an antenna operating between a PCS and a ground plane from the effective medium point of view. As a result, we have found that the cavity consisting of the PCS is an effectively low refractive index (n) medium, whose n is much lower than '1'. These kinds of media are generally known that they can increase gains or directivity of antennas [8]. Consequently, we will explain the high-gain property around the transparent frequency, at which the transmission through the PCS unit cell is the maximum, using the near-zero n behavior. All results were obtained using the commercial software of CST Microwave Studio (MWS) [9].

2. EFFECTIVE MEDIUM ANALYSIS

Consider the antenna structure given in Fig. 1. A simple dipole antenna is located between the frequency selective surface (FSS) superstrate and the infinite ground plane. The dipole axis is parallel to the x-direction. The superstrate consists of 11×23 cells in the xy-plane as shown in Fig. 1(b). The lateral dimension of the superstrate

is 126.5 mm × 132.3 mm, which corresponds to about $6\lambda \times 6.3\lambda$ at 14.3 GHz. The unit cell geometry of the FSS is also depicted in Fig. 1(c).

With the design shown in Fig. 1, we have optimized the performance of our antenna, and resulting antenna behaviors are presented in Fig. 2. The maximum realized gain is about 24.7 dB at 14.3 GHz, which is about 18 dB greater than that of an ideal dipole antenna above the same ground plane. Around the maximum radiation frequency, the antenna shows good impedance matching behavior, and the return loss is below −10 dB. The radiation patterns at 14.3 GHz are also shown in Fig. 2(b), which verifies the high-gain property of this antenna in comparison with that of the dipole antenna without the FSS superstrate. In Fig. 3, distribution of electric field strength at 14.3 GHz on the xy-plane located only 0.5 mm above the superstrate is shown in a dB scale. The field magnitude is strongest at the center of the superstrate, but the spread of the E-field strength is even throughout the entire superstrate. Therefore, we can see that the superstrate and substrate well perform a role as a cavity capturing an electromagnetic energy.

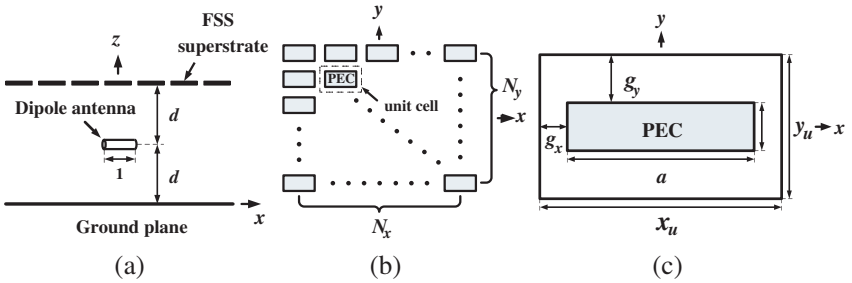

Figure 1. (a) Antenna geometry (side view) with $d = 5.5$ mm, $l = 3.5$ mm, (b) top view of the superstrate with $N_x = 11$, $N_y = 23$, (c) FSS superstrate unit cell geometry with $a = 10.5$ mm, $b = 1$ mm, $g_x = 0.5$ mm, $g_y = 2.375$ mm, $x_u = 11.5$ mm, and $y_u = 5.75$ mm.

In general, the phase relationship between the superstrate and substrate or reflection and transmission properties of an FSS superstrate is analyzed to explain the highly directive feature of cavity-resonant type antennas. However, this conventional method considering a resonance condition from the phase relationship provides a good approximation at only one resonant frequency. In other words, the resonance condition inside the cavity does not fully explain the high-gain feature around the resonant frequency region.

Thus, instead of following the conventional ways, we have tried

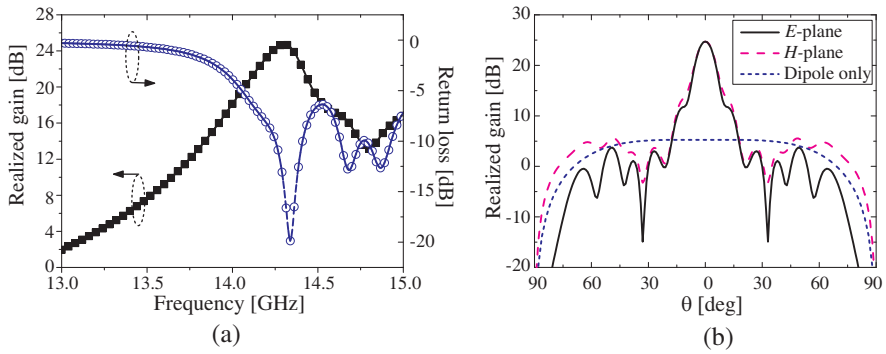

Figure 2. (a) Realized gain at $\theta = 0$ and a return loss, and (b) radiation patterns of the realized gain at the maximum gain frequency of 14.3 GHz.

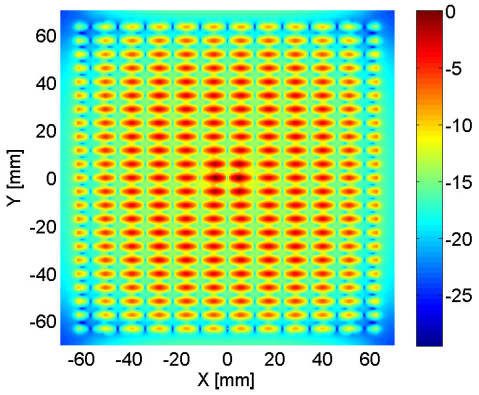

Figure 3. Distribution of electric field strength (dB-scale) on the xy-plane located 0.5 mm above the superstrate.

rather direct approach to investigate the high-gain feature of the cavity antenna by examining the properties of the cavity itself. We have considered the cavity as an effective medium, and have analyzed its electromagnetic properties.

Using an image theory, the unit cell of the cavity can be modeled as shown in Fig. 4. The ground plane is removed and the virtually mirrored image of the perfect electric conductor (PEC) plate is copied on the opposite side of the virtual ground plane. To excite an x-polarized plane wave, electric and magnetic boundary conditions are enforced on yz- and xz-planes, respectively.

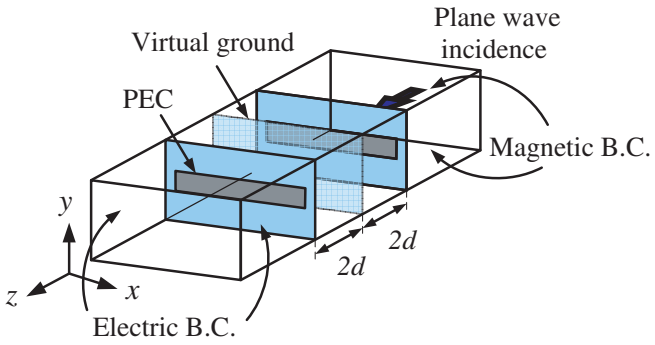

Figure 4. Equivalent cavity representation and a simulation setup for the retrieval of effective constitutive parameters.

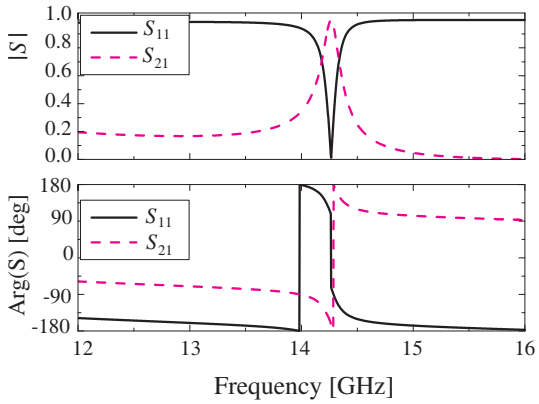

Figure 5. S parameters computed from the equivalent cavity model illustrated in Fig. 4.

Because our structure is symmetric with respect to the wave propagating direction, only S_{11} and S_{21} are needed to extract effective constitutive parameters, which are computed in Fig. 5. For the parameter retrieval, the relationship between a scattering matrix and

a refractive index and impedance has been used, which is written by

$$Z_n = \pm\sqrt{\frac{(1+S_{11})^2 - S_{21}^2}{(1-S_{11})^2 - S_{21}^2}} \tag{1}$$

$$n = \frac{\mathrm{Im}\left\{\ln\left(e^{i4nk_0d}\right)\right\} + 2m\pi \; - \; i\mathrm{Re}\left\{\ln\left(e^{i4nk_0d}\right)\right\}}{4k_0d} \tag{2}$$

$$e^{i4nk_0d} = \frac{S_{21}}{1 - S_{11}\frac{Z_n-1}{Z_n+1}} \tag{3}$$

where, n is an effective refractive index, k_0 is a propagation constant in free space, Z_n is impedance normalized by free space wave impedance, and m is an integer [10]. Im{} and Re{} indicate imaginary and real parts of {}, respectively. Since our cavity is a passive medium, Re$\{Z_n\}$ should be greater than or equal to 0. After Z_n is obtained by (1), the refractive index can be determined by (2) using the constraint condition of (3), whose magnitude always should be less than or equal to 1. Throughout the analysis, $e^{-i\omega t}$ time convention is assumed.

Figure 6 shows the retrieved constitutive parameters and impedance of the FSS cavity using the computed scattering parameters given in Fig. 5. It is very important to note that the maximum radiation gain shown in Fig. 2(a) is obtained at the frequency of $Z_n = 1$, i.e., 14.3 GHz. At this frequency, all energy transmits through the cavity and there is no reflection (see Fig. 5). Therefore, the cavity seems to be transparent, and its equivalent impedance is equal to that of free space, which is confirmed with the impedance behavior shown in Fig. 6.

To more precisely investigate the frequency of the maximum realized gain, we rewrite a well-known approximation of a resonant length ($2d$) of our antenna in terms of reflection phases of the superstrate and substrate, which is given by [5]

$$-\pi\left(\frac{16}{\lambda}d + 1\right) + \phi_r = 2N\pi \tag{4}$$

where, λ is a free space wavelength, ϕ_r is a reflection phase of the superstrate, and N is an integer. The frequency ($f_{G\max}$) yielding the maximum antenna gain, the frequency ($f_{Zn=1}$) of $Z_n = 1$, and the frequency (f_{cavity}) satisfying the condition (4) are compared in Fig. 7. In the figure, we see that (4) provides a reasonably good approximation of $f_{G\max}$. This agreement is quite well-known fact, but the consistence with $f_{Zn=1}$ is not. Again, Fig. 7 shows that the antenna gain is always maximum at $f_{Zn=1}$, hence, our analysis well satisfies (4) at least at one frequency equal to $f_{Zn=1}$.

However, (4) is satisfied at only one frequency of f_{cavity}. Therefore, when we examine a performance of an antenna at frequencies other than f_{cavity} (4) is no longer valid, and it is not easy to explain the reason of the high-gain feature shown in Fig. 2. Moreover, from Fig. 6, it can

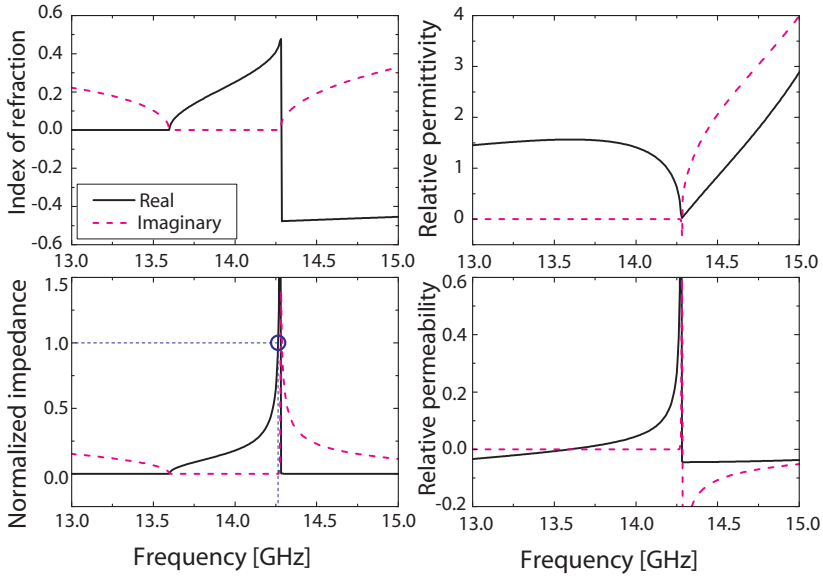

Figure 6. Retrieved effective constitutive parameters and normalized impedance of the structure depicted in Fig. 4.

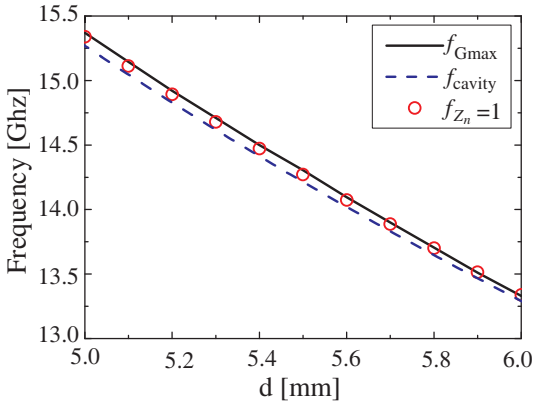

Figure 7. Comparison of the maximum radiation gain frequencies ($f_{G\max}$) and the frequencies ($f_{Zn} = 1$) of $Z_n = 1$ and the frequencies (f_{cavity}) satisfying (4) with respect to the variation of the cavity height d.

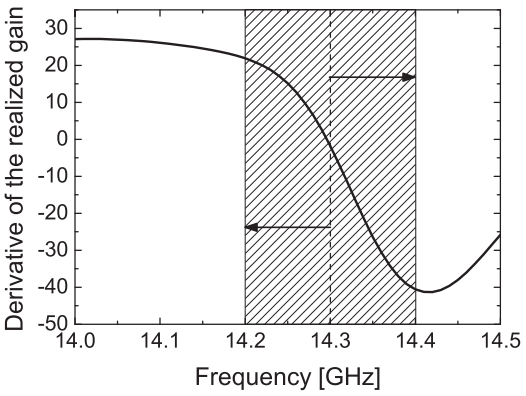

Figure 8. The derivative of the realized gain shown in Fig. 2(a).

be found that the impedance change is so dramatic within a narrow frequency band; for instance, Z_n is less than a quarter of free space wave impedance at 14.1 GHz. Notwithstanding the steep impedance variation, the gain curve shown in Fig. 2(a) drops rather slowly. This unusual gain behavior can be explained with the help of an effectively low n retrieved in Fig. 6. Within the frequency region of 13.6 GHz to 14.3 GHz, n varies from 0 to 0.47, which means that our cavity model can be considered as an effectively low n medium. Consequently, the gain property shown in Fig. 2, can be explained more clearly using this low effective n. Namely, the low n collimates waves toward the direction that is parallel to the surface normal direction, i.e., the z-direction, and pushes up the total antenna gain. There is another interesting frequency region beyond 14.3 GHz, in which the gain also decreases less sharply. In this frequency band, the magnitude of the real part of n is less than 0.5, which also can be considered as an effective medium with a low n. However, the imaginary part of $n(n'')$ starts to increase from 14.3 GHz. This loss is not large, but it impedes the growth of the antenna gain. Figure 8 shows the derivative of the antenna gain shown in Fig. 2(a). The effect of n'' on the gain behavior can be explained using the derivative of the realized gain within the matched impedance band of about 14.2 GHz to 14.4 GHz, where the return loss is less than -10 dB. From 14.2 GHz to 14.3 GHz, the average derivative of the realized gain with respect to the frequency is 13.9, but in the rest frequency band, it is -25.6, which is about twice larger in magnitude than the average derivative in the region of $n'' = 0$.

Figure 9 shows equivalent phase contours around the antenna at 14.0 GHz with and without the PRS superstrate. In Fig. 9(a), there is

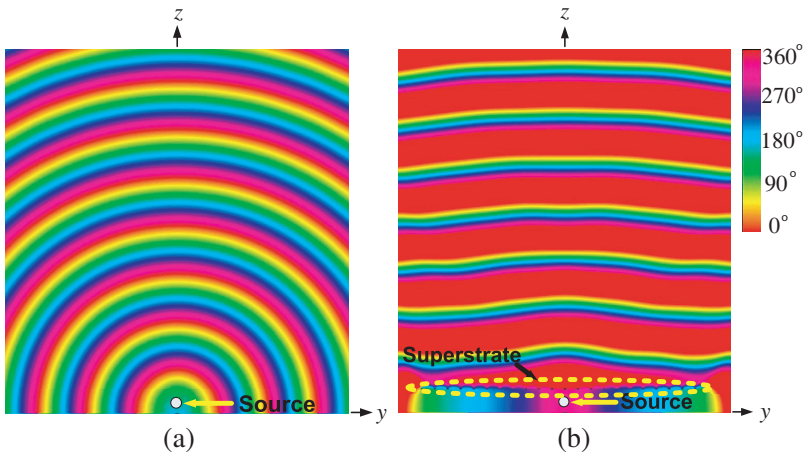

Figure 9. Equivalent phase contour plot at 14.0 GHz (a) without, and (b) with the FSS superstrate.

no scatterer around the source dipole antenna, and therefore, the phase contour exactly reflects wave-travelling path differences. However, in Fig. 9(b), the phase contour of the wave passed the superstrate looks like a straight line that is parallel to the y-axis. And, the outgoing wave is collimated toward the z-direction, as if there exists a slap with very low n around the feeding dipole antenna. Considering that the phase change from the source to the farthest element of the superstrate is larger than 6π, the collimation effect can be explained with the help of an effectively low n. This also agrees well with our analysis result shown in Fig. 6, and guarantees the validity of our effective medium analysis approach.

3. CONCLUSIONS

High-gain cavity type antenna has been investigated from a new viewpoint of an effective medium approach. We have shown that the Fabry-Pérot cavity increases an antenna gain not only for the satisfaction of a conventional cavity resonance condition, but also for the help of an effectively low index of refraction. Consequently, we have demonstrated that our approach can be used as another analysis method to explain the high-gain behavior of antenna around the cavity resonance frequency.

REFERENCES

1. Sirier, C., R. Cheype, R. Chantalat, M. Thevenot, T. Monediere, A. Reineix, and B. Jecko, "1-D photonic bandgap resonator antenna," *Microwave Opt. Tech. Lett.*, Vol. 29, No. 5, 312–315, Jun. 2001.
2. Ge, Y., K. P. Esselle, and Y. Hao, "Design of low-profile high-gain EBG resonator antennas using a genetic algorithm," *IEEE Antennas Wireless Propagat. Lett.*, Vol. 6, 480–483, 2007.
3. Pirhadi, A., F. Keshmiri, M. Hakkak, and M. Tayarani, "Analysis and design of dual band high directive EBG resonator antenna using square loop FSS as superstrate layer," *Progress In Electromagnetic Research*, PIER 70, 1–20, 2007.
4. Leger, L., R. Granger, M. Thevenot, T. Monediere, and B. Jecko, "Multifrequency dielectric EBG antenna," *Microwave Opt. Tech. Lett.*, Vol. 40, No. 5, 420–423, Mar. 2004.
5. Weily, A. R., T. S. Bird, and Y. H. Guo, "A reconfigurable high-gain partially reflecting surface antenna," *IEEE Trans. Antennas Propagat.*, Vol. 56, No. 11, 3382–3390, Nov. 2007.
6. Gardelli, R., M. Albani, and F. Capolino, "Array thinning by using antennas in a Fabry-Perot cavity for gain enhancement," *IEEE Trans. Antennas Propagat.*, Vol. 54, No. 7, 1979–1990, Jul. 2006.
7. Gu, Y. Y., W. X. Zhang, and Z. C. Ge, "Two improved Fabry-Perot resonator printed antennas using EBG superstrate and AMC substrate," *Journal of Electromagnetic Waves and Applications*, Vol. 41, No. 6, 719–728, 2007.
8. Wu, B.-I., W. Wang, J. Pacheco, X. Chen, J. Lu, T. M. Grzegorczyk, J. A. Kong, P. Kao, P. A. Theophelakes, and M. J. Hogan, "Anisotropic metamaterials as antenna substrate to enhance directivity," *Microwave Opt. Tech. Lett.*, Vol. 48, No. 4, 680–683, Apr. 2006.
9. *CST Microwave Studio: Workflow & Solver Overview*, CST Studio Suite 2008, CST-GmbH, 2008.
10. Smith, D. R., D. C. Vier, Th. Koschny, and C. M. Soukoulis, "Electromagnetic parameter retrieval from inhomogeneous metamaterials," *Physical Rev. E*, Vol. 71, 036617, 2005.